Journal of
Mechanics of
Materials and Structures

WAVE PROPAGATION IN LAYERED PIEZOELECTRIC RINGS WITH RECTANGULAR CROSS SECTIONS

JianGong Yu, XiaoDong Yang and Jean-Etienne Lefebvre

Volume 11, No. 3 May 2016

msp

JOURNAL OF MECHANICS OF MATERIALS AND STRUCTURES
Vol. 11, No. 3, 2016
dx.doi.org/10.2140/jomms.2016.11.245

WAVE PROPAGATION IN LAYERED PIEZOELECTRIC RINGS WITH RECTANGULAR CROSS SECTIONS

JIANGONG YU, XIAODONG YANG AND JEAN-ETIENNE LEFEBVRE

Wave propagation in multilayered piezoelectric structures has received much attention in past forty years. But the research objects of previous research works are almost only for semi-infinite structures and one-dimensional structures, i.e., structures with a finite dimension in only one direction, such as horizontally infinite flat plates and axially infinite hollow cylinders. This paper proposes a double orthogonal polynomial series approach to solve the wave propagation in a two-dimensional (2-D) layered piezoelectric structure, namely, a multilayered piezoelectric ring with a rectangular cross-section. Through numerical comparison with the available reference results for a purely elastic multilayered rectangular straight bar, the validity of the double polynomial series approach is illustrated. The dispersion curves and electric potential distributions of various layered piezoelectric rectangular rings with different material stacking directions, different polarization directions, different radius to thickness ratios, and different width to thickness ratios are calculated to reveal their wave propagation characteristics.

1. Introduction

Because of the applications in ultrasonic nondestructive evaluation and transducer design and optimization, wave propagation in multilayered piezoelectric structures has received considerable attention from engineering and scientific communities. Many solution methods have been used to investigate the wave propagation phenomena in multilayered piezoelectric structures. The mostly used method is the transfer matrix method (TMM) [Nayfeh 1995; Adler 2000; Cai et al. 2001] and the finite element method (FEM) [Ballandras et al. 2004]. Because the TMM and FEM suffer from numerical instability in some particular cases, some improvements have been developed, such as the recursive asymptotic stiffness matrix method [Wang and Rokhlin 2002; 2004], the surface impedance matrix method [Collet 2004; Zhang et al. 2001], the scattering-matrix method [Pastureaud et al. 2002] and the reverberation-ray matrix method [Guo et al. 2009].

The series expansion technique has been used for the problem of vibrations and waves. As early as 1960, Mindlin and McNiven [1960] used the Jacobi polynomial series to investigate the axially symmetric waves in elastic rods. Wu et al. [2014] also used the Jacobi polynomial series for the axially symmetric waves in piezoelectric ceramic rods. Dökmeci [1974] developed a double power series method to investigate the high frequency vibrations of piezoelectric crystal bars. Chou et al. [1991] used the double power series method for the dynamic analysis of a vibratory piezoelectric beam gyroscope. In 1972, an orthogonal polynomial approach has been developed to analyze linear acoustic waves in homogeneous semi-infinite wedges [Maradudin et al. 1972]. This approach has a special feature: it incorporates

Keywords: wave propagation, rectangular ring, piezoelectric materials, multilayered structures, double orthogonal polynomials.

the boundary conditions into the equations of motion. So the boundary conditions are automatically accounted for by assuming position-dependent material parameters. The equations of motion are then converted into a matrix eigenvalue problem through the expansion of the independent mechanical variables into appropriate series of orthonormal functions which makes the semivariational determination of the frequencies and the 8 associated modes possible. After that, this approach has been used to solve various wave propagation and vibration problems, including surface acoustic waves in layered semi-infinite piezoelectric structures [Datta and Hunsinger 1978; Kim and Hunt 1990], Lamb-like waves in multilayered piezoelectric plates [Lefebvre et al. 1999] and multilayered piezoelectric curved structures [Yu et al. 2013; 2012].

So far, investigations on wave propagation in multilayered piezoelectric structures are almost only for semi-infinite structures and one-dimensional structures, i.e., structures having a finite dimension in only one direction, such as horizontally infinite flat plates and axially infinite hollow cylinders. But in practical applications, many piezoelectric elements have finite dimensions in two directions, such as rings with rectangular cross sections. One-dimensional models are thus not suitable for these structures. This paper proposes a double orthogonal polynomial series approach to solve wave propagation in a 2-D piezoelectric structure, namely, a multilayered piezoelectric ring with rectangular cross-section. To the authors' knowledge, few references concerned on guided waves in multilayered piezoelectric rings. Two material stacking directions (radial direction and axial direction) and two polarization directions (also radial direction and axial direction) are respectively considered. The dispersion curves and the electric potential profiles of various layered piezoelectric rectangular rings are presented and discussed. In this paper, traction-free and open-circuit boundary conditions are assumed.

2. Problem formulation and solution method

We consider a multilayered piezoelectric ring with rectangular cross-section. In the cylindrical coordinate system (θ, z, r), a, b are the inner and outer radii. Figure 1 shows the schematic diagram of a multilayered ring with its stacking direction being in the axial direction. Its width is d, and the total height is $h = h_N$. The radius to thickness ratio is defined as $\eta = b/(b-a)$.

For the wave propagation problem considered in this paper, the body forces and electric charges are assumed to be zero. The dynamic wave equations are

$$\begin{aligned}
\frac{\partial T_{rr}}{\partial r} + \frac{1}{r}\frac{\partial T_{r\theta}}{\partial \theta} + \frac{\partial T_{rz}}{\partial z} + \frac{T_{rr} - T_{\theta\theta}}{r} &= \rho \frac{\partial^2 u_r}{\partial t^2} \\
\frac{\partial T_{r\theta}}{\partial r} + \frac{1}{r}\frac{\partial T_{\theta\theta}}{\partial \theta} + \frac{\partial T_{\theta z}}{\partial z} + \frac{2T_{r\theta}}{r} &= \rho \frac{\partial^2 u_\theta}{\partial t^2} \\
\frac{\partial T_{rz}}{\partial r} + \frac{1}{r}\frac{\partial T_{\theta z}}{\partial \theta} + \frac{\partial T_{zz}}{\partial z} + \frac{T_{rz}}{r} &= \rho \frac{\partial^2 u_z}{\partial t^2} \\
\frac{\partial D_r}{\partial r} + \frac{1}{r}\frac{\partial D_\theta}{\partial \theta} + \frac{\partial D_z}{\partial z} + \frac{D_r}{r} &= 0
\end{aligned} \tag{1}$$

where T_{ij}, u_i, and D_i are the stress, elastic displacement, and electric displacement components, respectively, and ρ is the density of the material.

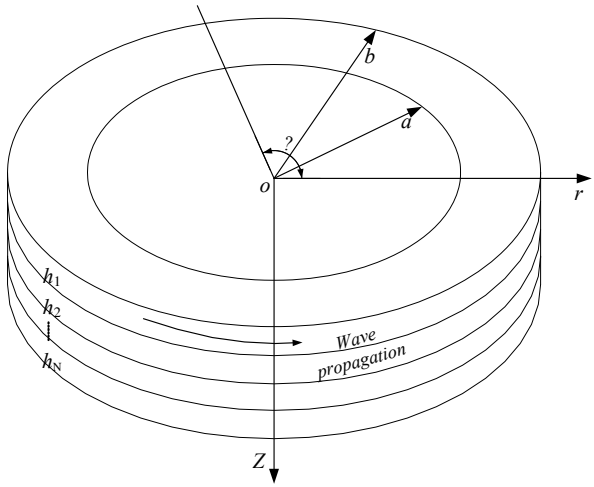

Figure 1. Schematic diagram of a z-direction multilayered rectangular ring.

The relationships between the generalized strain and generalized displacement components can be expressed as

$$\begin{aligned}
&\epsilon_{rr} = \frac{\partial u_r}{\partial r}, && \epsilon_{\theta\theta} = \frac{1}{r}\frac{\partial u_\theta}{\partial \theta} + \frac{u_r}{r}, && \epsilon_{zz} = \frac{\partial u_z}{\partial z},\\
&\epsilon_{\theta z} = \frac{1}{2}\left(\frac{\partial u_\theta}{\partial z} + \frac{\partial u_z}{r\partial \theta}\right), && \epsilon_{rz} = \frac{1}{2}\left(\frac{\partial u_r}{\partial z} + \frac{\partial u_z}{\partial r}\right), && \epsilon_{r\theta} = \frac{1}{2}\left(\frac{1}{r}\frac{\partial u_r}{\partial \theta} + \frac{\partial u_\theta}{\partial r} - \frac{u_\theta}{r}\right)\\
&E_r = -\frac{\partial \phi}{\partial r}, && E_\theta = -\frac{1}{r}\frac{\partial \phi}{\partial \theta}, && E_z = -\frac{\partial \phi}{\partial z},
\end{aligned} \tag{2}$$

where ϵ_{ij}, E_i, and ϕ are the strain components, electric field, and electric potential, respectively.

In this paper, we consider two kinds of layered piezoelectric rings, namely the material stacking direction being respectively in the radial direction and in the axial direction. For a ring with a material stacking direction being in the axial direction, we denote it as a-directional layered ring. Its elastic parameters are expressed as

$$\begin{aligned}
C_{ij} &= \sum_{n=1}^{N} C_{ij}^n \pi_{h_{n-1},h_n}(z), \quad e_{ij} = \sum_{n=1}^{N} e_{ij}^n \pi_{h_{n-1},h_n}(z),\\
\in_{ij} &= \sum_{n=1}^{N} \in_{ij}^n \pi_{h_{n-1},h_n}(z), \qquad \rho = \sum_{n=1}^{N} \rho^n \pi_{h_{n-1},h_n}(z)
\end{aligned} \tag{3}$$

where

$$\pi_{h_{n-1},h_n}(z) = \begin{cases} 1, & h_{n-1} \le z \le h_n,\\ 0, & \text{elsewhere;} \end{cases}$$

N is the number of the layers and C_{ij}^n, e_{ij}^n, $\in_{ij}^n$ are the elastic, piezoelectric and dielectric constants of the n-th layer.

For a layered ring with a stacking direction being in the radial direction, we denote it as r-directional layered ring. Its material constants are expressed as

$$\begin{aligned} C_{ij} &= \sum_{n=1}^{N} C_{ij}^{n}\pi_{d_{n-1},d_n}(r), \quad e_{ij} = \sum_{n=1}^{N} e_{ij}^{n}\pi_{d_{n-1},d_n}(r), \\ \in_{ij} &= \sum_{n=1}^{N} \in_{ij}^{n}\pi_{d_{n-1},d_n}(r), \qquad \rho = \sum_{n=1}^{N} \rho^{n}\pi_{d_{n-1},d_n}(r) \end{aligned} \tag{4}$$

where

$$\pi_{d_{n-1},d_n}(z) = \begin{cases} 1, & d_{n-1} \le r \le d_n, \\ 0, & \text{elsewhere.} \end{cases}$$

Simultaneously, two different polarization directions, i.e., radially polarized direction and axially polarized direction, will be considered. We use "Pr" and "Pa" to represent the two different polarization directions.

We introduce the function $I(r, z)$

$$I(r, z) = \pi(r)\pi(z) = \begin{cases} 1, & a \le r \le b \text{ and } 0 \le z \le h, \\ 0, & \text{elsewhere,} \end{cases} \tag{5}$$

where $\pi(r)$ and $\pi(z)$ are rectangular window functions (the subtraction of two Heaviside function)

$$\pi(r) = \begin{cases} 1, & a \le r \le b, \\ 0, & \text{elsewhere,} \end{cases} \quad \text{and} \quad \pi(z) = \begin{cases} 1, & 0 \le z \le h, \\ 0, & \text{elsewhere.} \end{cases}$$

The derivatives along r and z of $I(r, z)$ are

$$\frac{\partial I(r, z)}{\partial r} = \delta(r - a) - \delta(r - b) \quad \text{and} \quad \frac{\partial I(r, z)}{\partial z} = \delta(z) - \delta(z - h).$$

By introducing the function $I(r, z)$, the traction-free and open-circuit boundary conditions — that is, $T_{rr} = T_{r\theta} = T_{rz} = T_{\theta z} = T_{zz} = D_r = D_z = 0$ at the four boundaries — are automatically incorporated in the constitutive relations of the ring [Ludwig and Lengeler 1964]:

$$\begin{Bmatrix} T_{\theta\theta} \\ T_{zz} \\ T_{rr} \\ T_{rz} \\ T_{r\theta} \\ T_{\theta z} \end{Bmatrix} = \begin{bmatrix} C_{11} & C_{12} & C_{13} & C_{14} & C_{15} & C_{16} \\ & C_{22} & C_{23} & C_{24} & C_{25} & C_{26} \\ & & C_{33} & C_{34} & C_{35} & C_{36} \\ & & & C_{44} & C_{45} & C_{46} \\ & \text{symmetry} & & & C_{55} & C_{56} \\ & & & & & C_{66} \end{bmatrix} \begin{Bmatrix} \epsilon_{\theta\theta} I(r, z) \\ \epsilon_{zz} I(r, z) \\ \epsilon_{rr} I(r, z) \\ 2\epsilon_{rz} I(r, z) \\ 2\epsilon_{r\theta} I(r, z) \\ 2\epsilon_{\theta z} I(r, z) \end{Bmatrix} - \begin{bmatrix} e_{11} & e_{21} & e_{31} \\ e_{12} & e_{22} & e_{32} \\ e_{13} & e_{23} & e_{33} \\ e_{14} & e_{24} & e_{34} \\ e_{15} & e_{25} & e_{35} \\ e_{16} & e_{26} & e_{36} \end{bmatrix} \begin{Bmatrix} E_\theta I(r, z) \\ E_z I(r, z) \\ E_r I(r, z) \end{Bmatrix} \tag{6a}$$

$$\begin{Bmatrix} D_\theta \\ D_z \\ D_r \end{Bmatrix} = \begin{bmatrix} e_{11} & e_{12} & e_{13} & e_{14} & e_{15} & e_{16} \\ e_{21} & e_{22} & e_{23} & e_{24} & e_{25} & e_{26} \\ e_{31} & e_{32} & e_{33} & e_{34} & e_{35} & e_{36} \end{bmatrix} \begin{Bmatrix} \epsilon_{\theta\theta} I(r, z) \\ \epsilon_{zz} I(r, z) \\ \epsilon_{rr} I(r, z) \\ 2\epsilon_{rz} I(r, z) \\ 2\epsilon_{r\theta} I(r, z) \\ 2\epsilon_{\theta z} I(r, z) \end{Bmatrix} + \begin{bmatrix} \in_{11} & \in_{12} & \in_{13} \\ & \in_{22} & \in_{23} \\ \text{symmetry} & & \in_{33} \end{bmatrix} \begin{Bmatrix} E_\theta I(r, z) \\ E_z I(r, z) \\ E_r I(r, z) \end{Bmatrix}. \tag{6b}$$

For a time-harmonic wave propagating in the circumferential direction of a ring, we assume the displacement components to be of the form

$$\begin{aligned} u_r(r,\theta,z,t) &= \exp(ikb\theta - i\omega t)\,U(r,z), \quad u_\theta(r,\theta,z,t) = \exp(ikb\theta - i\omega t)\,V(r,z), \\ u_z(r,\theta,z,t) &= \exp(ikb\theta - i\omega t)\,W(r,z), \quad \psi(r,\theta,z,t) = \exp(ikb\theta - i\omega t)\,X(r,z), \end{aligned} \tag{7}$$

where $U(r,z)$, $V(r,z)$, and $W(r,z)$ represent the amplitude of vibration in the r, θ, z directions, respectively, and $X(r,z)$ represents the amplitude of electric potential. Also, k is the magnitude of the wave vector in the propagation direction, and ω is the angular frequency.

Substituting (2), (6), and (7) into (1), the governing differential equations in terms of the displacement and the electric potential components can be obtained. In the case of Pr r-directional layered orthotropic ring, they are given by

$$\begin{aligned} \sum_{n=1}^{N}\Big\{&[C_{33}^n(r^2U_{,rr}+rU_{,r}) - (C_{11}^n+(kb)^2C_{55}^n)U + C_{44}^n r^2U_{,zz} + ikb(C_{13}^n+C_{55}^n)rV_{,r} \\ &- ikb(C_{11}^n+C_{55}^n)V + (C_{23}^n+C_{44}^n)r^2W_{,rz} + (C_{23}^n-C_{12}^n)rW_{,z} + e_{33}^n(r^2X_{,rr}+rX_{,r}) + e_{24}^n r^2X_{,zz} \\ &- (kb)^2e_{15}^nX - e_{31}^nrX_{,r}]\pi_{d_{n-1},d_n}(r)\cdot\pi(z) + [C_{44}^nr^2(U_{,z}+W_{,r}) + e_{24}^nr^2X_{,z}]\pi_{d_{n-1},d_n}(r)\cdot\pi(z)_{,z} \\ &+ [C_{33}^nr^2U_{,r} + C_{13}^nr(ikbV+U) + C_{23}^nr^2W_{,z} + e_{33}^nr^2X_{,r}]\pi_{d_{n-1},d_n}(r)_{,r}\cdot\pi(z)\Big\} \\ &= -\sum_{n=1}^{N}\rho^n\pi_{d_{n-1},d_n}(r)r^2\omega^2U\cdot\pi(z), \end{aligned} \tag{8a}$$

$$\begin{aligned} \sum_{n=1}^{N}\Big\{&[C_{55}^n(r^2V_{,rr}+rV_{,r}) - (C_{55}^n+(kb)^2C_{11}^n)V + ikb(C_{13}^n+C_{55}^n)rU_{,r} + ikb(C_{11}^n+C_{66}^n)U \\ &+ C_{66}^nr^2V_{,zz} + ikb(C_{12}^n+C_{66}^n)rW_{,z} + (e_{31}^n+e_{15}^n)rX_{,r} + 2e_{15}^nX]\pi_{d_{n-1},d_n}(r)\cdot\pi(z) \\ &+ C_{66}^n(r^2V_{,z} + ikbrW)\pi_{d_{n-1},d_n}(r)\cdot\pi(z)_{,z} \\ &+ [C_{55}^n(r^2V_{,r} + rV + ikbrU) + e_{15}^nrX]\pi_{d_{n-1},d_n}(r)_{,r}\cdot\pi(z)\Big\} \\ &= -\sum_{n=1}^{N}\rho^n\pi_{d_{n-1},d_n}(r)\cdot\pi(z)r^2\omega^2V, \end{aligned} \tag{8b}$$

$$\begin{aligned} \sum_{n=1}^{N}\Big\{&[C_{44}^n(r^2W_{,rr}+rW_{,r}) - (kb)^2C_{66}^nW + C_{22}^nr^2W_{,zz} + (C_{23}^n+C_{44}^n)r^2U_{,rz} + (C_{12}^n+C_{44}^n)rU_{,z} \\ &+ ikb(C_{12}^n+C_{66}^n)rV_{,z} + (e_{24}^n+e_{32}^n)r^2X_{,rz} + e_{24}^nrX_{,z}]\pi_{d_{n-1},d_n}(r)\cdot\pi(z) \\ &+ [C_{12}^nr(ikbV+U)C_{23}^nr^2U_{,r} + C_{22}^nr^2W_{,z} + e_{32}^nr^2X_{,r}]\pi_{d_{n-1},d_n}(r)\cdot\pi(z)_{,z} \\ &+ [C_{44}^nr^2(W_{,r}+U_{,z}) + e_{24}^nr^2X_{,z}]\pi_{d_{n-1},d_n}(r)_{,r}\cdot\pi(z)\Big\} \\ &= -\sum_{n=1}^{N}\rho^nr^2\omega^2V\pi_{d_{n-1},d_n}(r)\cdot\pi(z), \end{aligned} \tag{8c}$$

$$\sum_{n=1}^{N}\Big\{[e_{33}^{n}(r^2U_{,rr}+rU_{,r})+e_{31}^{n}rU_{,r}-(kb)^2e_{15}^{n}U+e_{24}^{n}r^2U_{,zz}-e_{15}^{n}V+(e_{31}^{n}+e_{15}^{n})rV_{,r}+e_{24}^{n}rW_{,z}$$
$$+(e_{24}^{n}+e_{32}^{n})r^2W_{,rz}+(kb)^2\epsilon_{11}^{n}X-\epsilon_{33}^{n}(r^2X_{,rr}+rX_{,r})-\epsilon_{22}^{n}r^2X_{,zz}]\pi_{d_{n-1},d_n}(r)\cdot\pi(z)$$
$$+[e_{33}^{n}r^2U_{,r}+e_{31}^{n}rU+e_{31}^{n}rV+e_{32}^{n}r^2W_{,z}-\epsilon_{33}^{n}r^2X_{,r}]\pi_{d_{n-1},d_n}(r)_{,r}\cdot\pi(z)$$
$$+[e_{24}^{n}r^2U_{,z}+e_{24}^{n}r^2W_{,r}-\epsilon_{22}^{n}r^2X_{,z}]\pi_{d_{n-1},d_n}(r)\cdot\pi(z)_{,z}\Big\}$$
$$=0. \tag{8d}$$

where a subscript comma indicates partial derivative.

To solve the coupled wave equation, $U(r,z)$, $V(r,z)$, $W(r,z)$, and $X(r,z)$ are expanded into products of two Legendre orthogonal polynomial series as

$$\begin{aligned} U(r,z)&=\sum_{m,j=0}^{\infty}p_{m,j}^{1}Q_m(r)Q_j(z), & V(r,z)&=\sum_{m,j=0}^{\infty}p_{m,j}^{2}Q_m(r)Q_j(z),\\ W(r,z)&=\sum_{m,j=0}^{\infty}p_{m,j}^{3}Q_m(r)Q_j(z), & X(r,z)&=\sum_{m,j=0}^{\infty}p_{m,j}^{4}Q_m(r)Q_j(z), \end{aligned} \tag{9}$$

where $p_{m,j}^{i}$ $(i=1,2,3,4)$ are the expansion coefficients and

$$Q_m(r)=\sqrt{\frac{2m+1}{b-a}}P_m\left(\frac{2r-b-a}{b-a}\right), \qquad Q_j(z)=\sqrt{\frac{2j+1}{h}}P_j\left(\frac{2z-h}{h}\right) \tag{10}$$

with P_m and P_j being the m-th and the j-th Legendre polynomial. Theoretically, m and j run from 0 to ∞. However, in practice the summation over the polynomials in (9) can be truncated at some finite values $m=M$ and $j=J$, when the effects of higher order terms become negligible.

Equations (8) are multiplied by $Q_n(r)$ with n running from 0 to M, and by $Q_p(z)$ with p from 0 to J, respectively. Then integrating over z from 0 to h and over r from a to b gives the following system of linear algebraic equations:

$$ {}^{l}A_{11}^{n,p,m,j}p_{m,j}^{1}+{}^{l}A_{12}^{n,p,m,j}p_{m,j}^{2}+{}^{l}A_{13}^{n,p,m,j}p_{m,j}^{3}+{}^{l}A_{14}^{n,p,m,j}p_{m,j}^{4}=-\omega^2\cdot{}^{l}M_{n,p,m,j}p_{m,j}^{1}, \tag{11a}$$
$$ {}^{l}A_{21}^{n,p,m,j}p_{m,j}^{1}+{}^{l}A_{22}^{n,p,m,j}p_{m,j}^{2}+{}^{l}A_{23}^{n,p,m,j}p_{m,j}^{3}+{}^{l}A_{24}^{n,p,m,j}p_{m,j}^{4}=-\omega^2\cdot{}^{l}M_{n,p,m,j}p_{m,j}^{2}, \tag{11b}$$
$$ {}^{l}A_{31}^{n,p,m,j}p_{m,j}^{1}+{}^{l}A_{32}^{n,p,m,j}p_{m,j}^{2}+{}^{l}A_{33}^{n,p,m,j}p_{m,j}^{3}+{}^{l}A_{34}^{n,p,m,j}p_{m,j}^{4}=-\omega^2\cdot{}^{l}M_{n,p,m,j}p_{m,j}^{3}, \tag{11c}$$
$$ {}^{l}A_{41}^{n,p,m,j}p_{m,j}^{1}+{}^{l}A_{42}^{n,p,m,j}p_{m,j}^{2}+{}^{l}A_{43}^{n,p,m,j}p_{m,j}^{3}+{}^{l}A_{44}^{n,p,m,j}p_{m,j}^{4}=0, \tag{11d}$$

where ${}^{l}A_{\alpha\beta}^{n,p,m,j}$ $(\alpha,\beta=1,2,3,4)$ and ${}^{l}M_{n,p,m,j}$ are the elements of the nonsymmetric matrices $\boldsymbol{A}$ and $\boldsymbol{M}$, which can be obtained by using (8).

Equation (11d) can be written as

$$p_{m,j}^{4}=-\left({}^{l}A_{44}^{n,p,m,j}\right)^{-1}\left({}^{l}A_{41}^{n,p,m,j}p_{m,j}^{1}+{}^{l}A_{42}^{n,p,m,j}p_{m,j}^{2}+{}^{l}A_{43}^{n,p,m,j}p_{m,j}^{3}\right). \tag{12}$$

Substituting (12) into (11a)–(11c) gives

$$\begin{aligned}
&\left[{}^{l}A_{11}^{n,p,m,j} - {}^{l}A_{14}^{n,p,m,j}\left({}^{l}A_{44}^{n,p,m,j}\right)^{-1}\cdot {}^{l}A_{41}^{n,p,m,j}\right]p_{m,j}^{1}\\
&+\left[{}^{l}A_{12}^{n,p,m,j} - {}^{l}A_{14}^{n,p,m,j}\left({}^{l}A_{44}^{n,p,m,j}\right)^{-1}\cdot {}^{l}A_{42}^{n,p,m,j}\right]p_{m,j}^{2}\\
&+\left[{}^{l}A_{13}^{n,p,m,j} - {}^{l}A_{14}^{n,p,m,j}\left({}^{l}A_{44}^{n,p,m,j}\right)^{-1}\cdot {}^{l}A_{43}^{n,p,m,j}\right]p_{m,j}^{3} = -\omega^{2l}M_{n,p,m,j}\,p_{m,j}^{1}, \qquad (13a)\\
&\left[{}^{l}A_{21}^{n,p,m,j} - {}^{l}A_{24}^{n,p,m,j}\left({}^{l}A_{44}^{n,p,m,j}\right)^{-1}\cdot {}^{l}A_{41}^{n,p,m,j}\right]p_{m,j}^{1}\\
&+\left[{}^{l}A_{22}^{n,p,m,j} - {}^{l}A_{24}^{n,p,m,j}\left({}^{l}A_{44}^{n,p,m,j}\right)^{-1}\cdot {}^{l}A_{42}^{n,p,m,j}\right]p_{m,j}^{2}\\
&+\left[{}^{l}A_{23}^{n,p,m,j} - {}^{l}A_{24}^{n,p,m,j}\left({}^{l}A_{44}^{n,p,m,j}\right)^{-1}\cdot {}^{l}A_{43}^{n,p,m,j}\right]p_{m,j}^{3} = -\omega^{2l}M_{n,p,m,j}\,p_{m,j}^{2}, \qquad (13b)\\
&\left[{}^{l}A_{31}^{n,p,m,j} - {}^{l}A_{34}^{n,p,m,j}\left({}^{l}A_{44}^{n,p,m,j}\right)^{-1}\cdot {}^{l}A_{41}^{n,p,m,j}\right]p_{m,j}^{1}\\
&+\left[{}^{l}A_{32}^{n,p,m,j} - {}^{l}A_{34}^{n,p,m,j}\left({}^{l}A_{44}^{n,p,m,j}\right)^{-1}\cdot {}^{l}A_{42}^{n,p,m,j}\right]p_{m,j}^{2}\\
&+\left[{}^{l}A_{33}^{n,p,m,j} - {}^{l}A_{34}^{n,p,m,j}\left({}^{l}A_{44}^{n,p,m,j}\right)^{-1}\cdot {}^{l}A_{43}^{n,p,m,j}\right]p_{m,j}^{3} = -\omega^{2l}M_{n,p,m,j}\,p_{m,j}^{3}. \qquad (13c)
\end{aligned}$$

Then, (11) can be rewritten as

$$\begin{bmatrix} {}^{l}\bar{A}_{11}^{n,p,m,j} & {}^{l}\bar{A}_{12}^{n,p,m,j} & {}^{l}\bar{A}_{13}^{n,p,m,j} \\ {}^{l}\bar{A}_{21}^{n,p,m,j} & {}^{l}\bar{A}_{22}^{n,p,m,j} & {}^{l}\bar{A}_{22}^{n,p,m,j} \\ {}^{l}\bar{A}_{31}^{n,p,m,j} & {}^{l}\bar{A}_{32}^{n,p,m,j} & {}^{l}\bar{A}_{33}^{n,p,m,j} \end{bmatrix} \begin{Bmatrix} p_{m,j}^{1} \\ p_{m,j}^{2} \\ p_{m,j}^{3} \end{Bmatrix} = -\omega^{2l}M_{n,p,m,j} \begin{bmatrix} 1 & 0 & 0 \\ 0 & 1 & 0 \\ 0 & 0 & 1 \end{bmatrix} \begin{Bmatrix} p_{m,j}^{1} \\ p_{m,j}^{2} \\ p_{m,j}^{3} \end{Bmatrix}. \qquad (14)$$

So, (14) forms the eigenvalue problem to be solved. The eigenvalues ω^2 give the angular frequency of the guided wave modes, and the eigenvectors $p_{m,j}^{i}$ $(i = 1, 2, 3)$ allow the mechanical displacement components to be calculated, and $p_{m,j}^{4}$, which can be obtained from (12), determines the electric potential distribution. By using the relation $Vph = \omega/k$, the phase wave velocity Vph can be obtained. In the computing progress, the obtained eigenvalues are complex, but their imaginary parts are all very small compared to their corresponding real parts. For one eigenvalue, its imaginary part is less than one millionth of its real part. So, we just think the real parts are solutions of the system.

3. Numerical results and discussions

Based on the solution procedure as described in Section 2, a computer program in terms of the extended polynomial approach has been written using Mathematica to calculate the wave dispersion curves, the displacement and the electric potential distributions for the layered piezoelectric rectangular rings.

3.1. ***Comparison with the available solution from the transfer matrix method.*** Since no reference results for the wave dispersion curves in layered piezoelectric rectangular rings can be found in literature, we consider an a-direction layered purely elastic rectangular ring with a very large radius to thickness ratio ($\eta = 1000$) to make a comparison with known results of a straightly layered bar from the semi-analytical finite element method [Taweel et al. 2000]. It is a three layer $+30°/-30°/+30°$ (with respect to the θ-axis) fiber composite rectangular ring with equal layer-thickness. The bar's width-to-height ratio is $d/h = 2$ and the material properties are given by (15) [loc. cit.]. Figure 2 shows the corresponding dispersion curves, in which the solid lines are from [loc. cit.], and the dotted lines are obtained from the

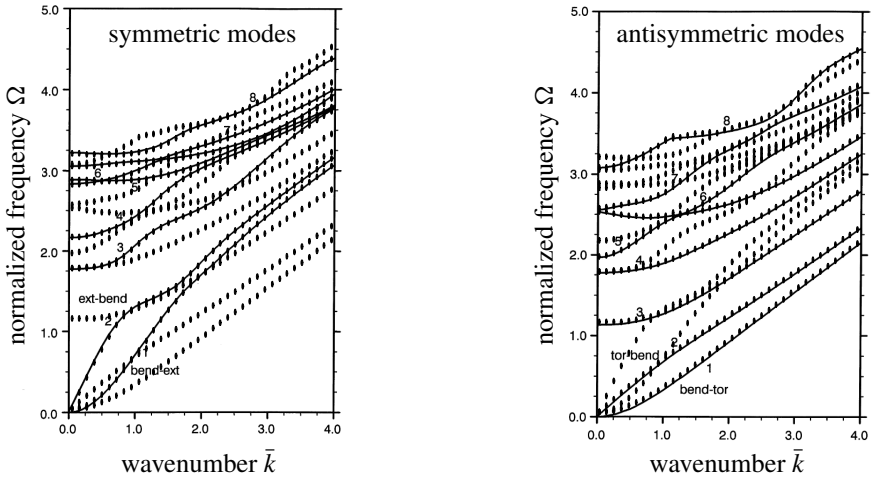

Figure 2. Dispersion curves for the three-layer $[+30°/-30°/+30°]$, equal thickness fiber composite rectangular structures. Solid lines: the results from the semi-analytical FEM [Taweel et al. 2000] for the straightly layered bar; dotted lines: the results of the presented method for the layered ring with a very large radius to thickness ratio ($\eta = 1000$).

proposed polynomial approach. The normalized frequency is defined by $\omega/\sqrt{15.167\,\text{GPa}/\rho h^2}$, and the dimensionless wave number kh is introduced. In [Taweel et al. 2000], all wave modes are assorted into two classes and shown in two separate figures. But the proposed method in this paper can only calculate all wave modes together. So, we put the dispersion curves of all wave modes in each figure to make the comparison. As can be seen, the results from the proposed polynomial approach agree very well with the available reference data.

$$[C]_{\pm 30^\circ} = \begin{bmatrix} 86.231 & 27.5875 & 3.9233 & 0 & 0 & \mp 40.6352 \\ & 23.73 & 3.6078 & 0 & 0 & \mp 13.4923 \\ & & 15.986 & 0 & 0 & \mp 0.2732 \\ & & & 6.1663 & 0 & 0 \\ & \text{symmetry} & & & 5.9628 & 0 \\ & & & & & 29.3675 \end{bmatrix} \text{GPa}. \tag{15}$$

3.2. ***Dispersion curves in multilayered piezoelectric rectangular rings.*** In this section, layered piezoelectric rectangular rings composed of BSN (B) and PZT-4 (P) are studied. The corresponding material parameters can be seen in [Guo et al. 2009]. Here, the elastic constants of r-polarization and a-polarization are taken as the same in order to make appropriate comparisons.

Firstly, four square rings with $\eta = 10$ are considered. Their stacking sequences, thickness ratio are the same, P/B/P-1/1/1. Their stacking directions and polarization directions are different: (a) is a Pr r-directional layered ring; (b) is a Pr a-directional layered ring; (c) is a Pa r-directional layered ring; (d) is a Pa a-directional layered ring. Their phase velocity dispersion curves are shown in Figure 3. It can be seen that both the stacking direction and the polarization direction have influences on the dispersion curves.

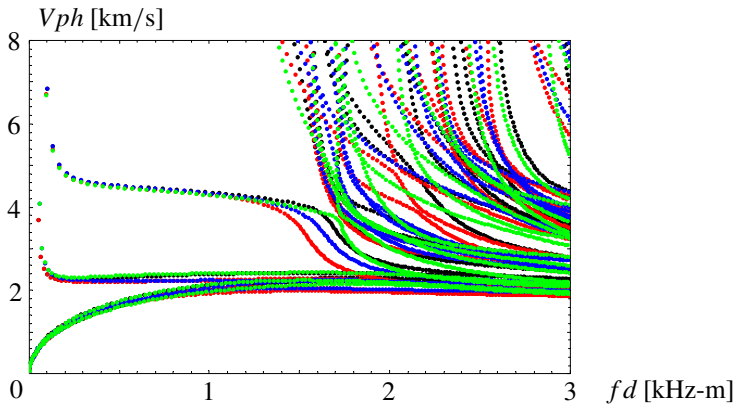

Figure 3. Phase velocity dispersion curves for the P/B/P-1/1/1 square rings with $\eta = 10$. Layered rings: Pa a-directional (red), Pa r-directional (green), Pr a-directional (black), and Pr r-directional (blue).

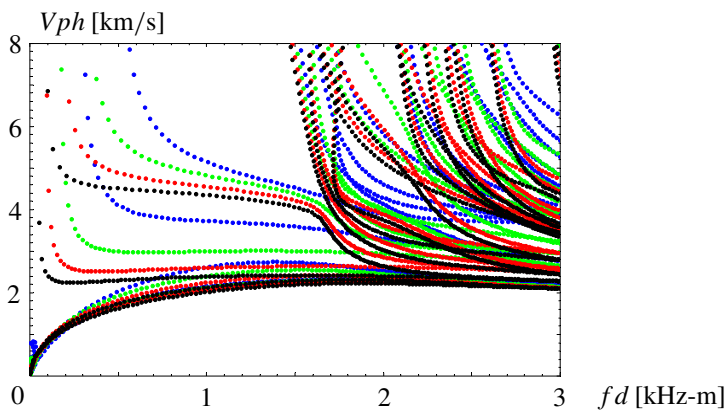

Figure 4. Phase velocity dispersion curves for r-polarized and a-directional P/B/P-1/1/1 square rings: $\eta = 2$ (blue), $\eta = 3$ (green), $\eta = 5$ (red), and $\eta = 10$ (black).

Then, Figure 4 shows the dispersion curves for r-polarized and a-directional P/B/P-1/1/1 square rings with different radius to thickness ratios, $\eta = 2, 3, 5$, and 10, respectively. Obviously, the radius to thickness ratio has significant influences on the dispersion curves.

Next, the different stacking sequences are discussed. Phase velocity dispersion curves for three r-polarized and r-directional thickness-equal rectangular rings with $\eta = 2$ and $d/h = 0.5$ are shown in Figure 5. Their stacking sequences are B/P/P, P/B/P, and P/P/B. On the whole, the phase velocity of B/P/P ring is the lowest and that of P/P/B ring is the highest. In fact, the wave velocity of BSN is higher than that of PZT-4. Moreover, the volume fraction of BSN in B/P/P ring is the lowest in the three r-directional layered rings because of its BSN being located at the innermost layer. When the radius to thickness ratio becomes smaller, the difference among the volume factions of the three r-directional

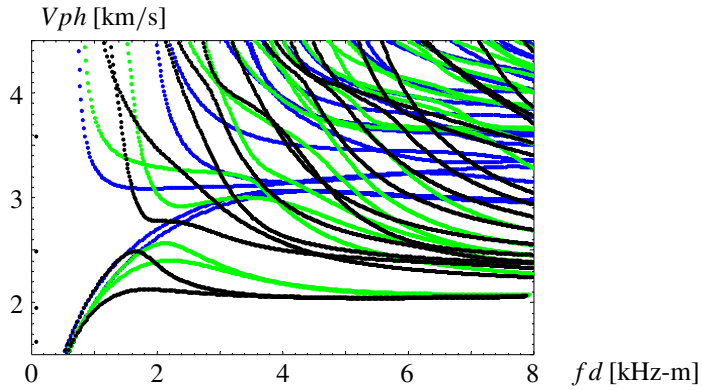

Figure 5. Phase velocity dispersion curves for r-polarized and r-directional thickness equal rectangular rings with $\eta = 2$ and $d/h = 0.5$: B/P/P (black), P/B/P (green), and P/P/B (blue).

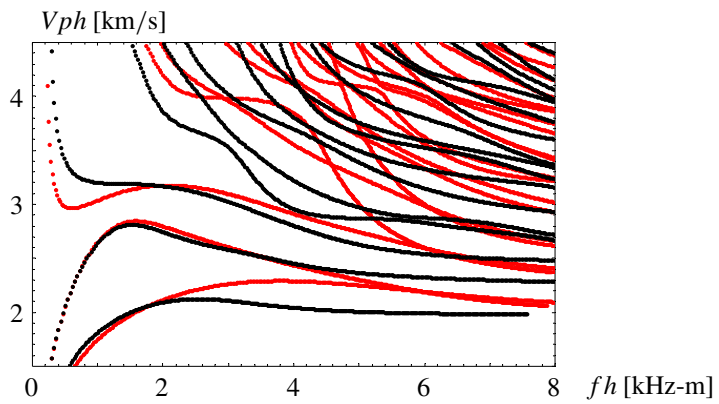

Figure 6. Phase velocity dispersion curves for r-polarized and a-directional thickness equal rectangular rings with $\eta = 2$ and $d/h = 2$: P/B/P (red) and P/P/B (black).

layered rings becomes larger. For a-directional layered rings, the volume fractions of P/B/P-1/1/1 and P/P/B-1/1/1 rings are the same, but different stacking sequence still results in different dispersion curves, as shown in Figure 6.

3.3. ***Displacement and electric potential shapes.*** This section discusses the wave characteristics of layered square rings through the displacement and the electric potential shapes. The displacement in wave propagating direction and the electric potential shapes at $kd = 30.3$ of the fourth and seventh modes for Pr a-directional layered square ring are illustrated in Figure 7. It can be seen that the displacement and the electric potential are always concentrated near the four boundaries. Furthermore, they are mostly localized in the layers of PZT-4, which has a lower wave speed than BSN. In order to confirm this phenomenon, the top of Figure 8 shows the seventh mode of the Pr a-directional B/P/B-1/1/1 square ring with $\eta = 10$ at $kd = 30.3$. The displacement and the electric potential are mostly localized in the middle layer, the layer of PZT-4. Finally, the bottom of Figure 8 shows, for the case of small radius

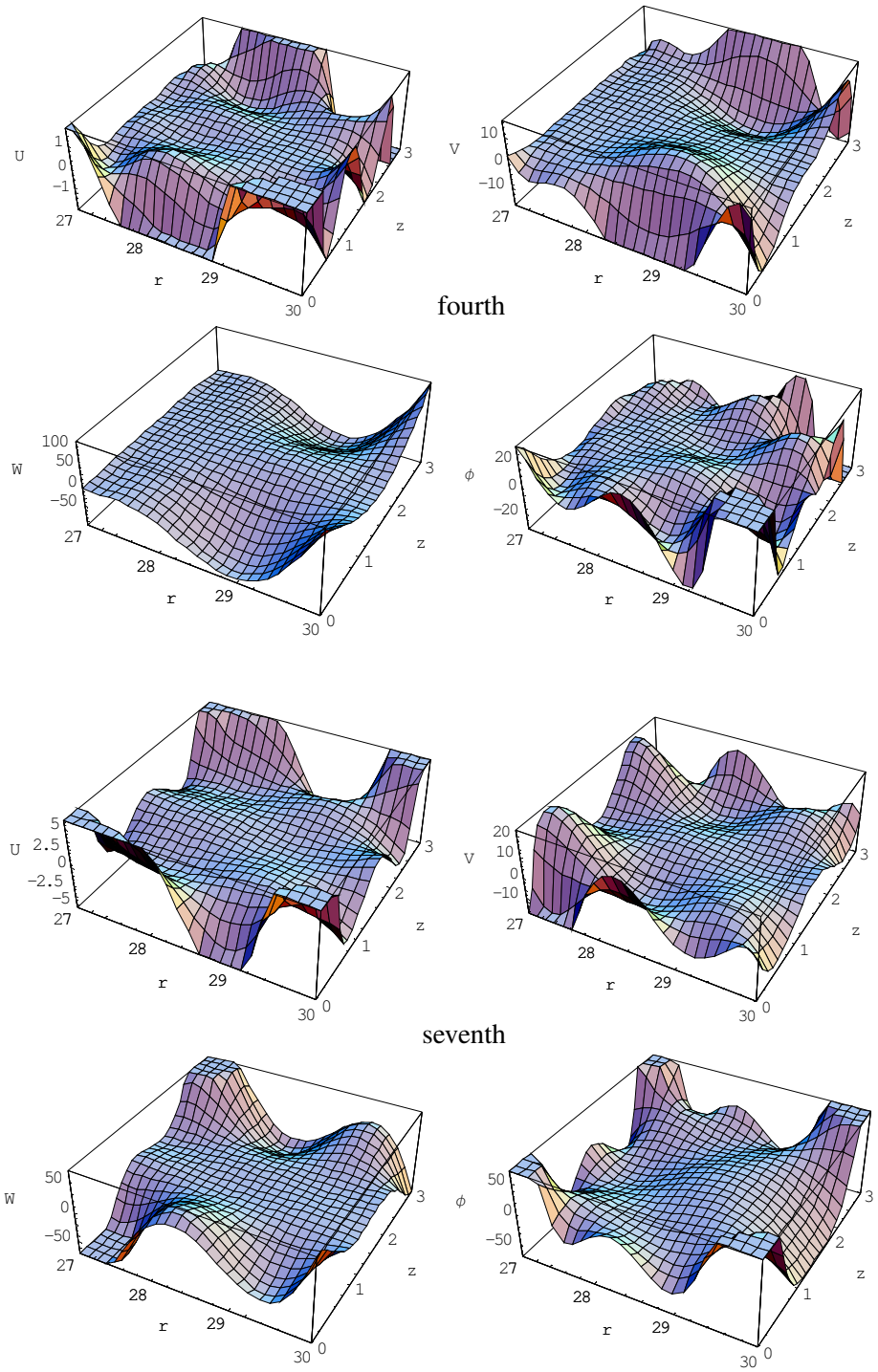

Figure 7. Displacement and electric potential profiles of the fourth mode (top) and seventh mode (bottom) for the Pr a-directional P/B/P-1/1/1 square ring with $\eta = 10$ at $kd = 30.3$.

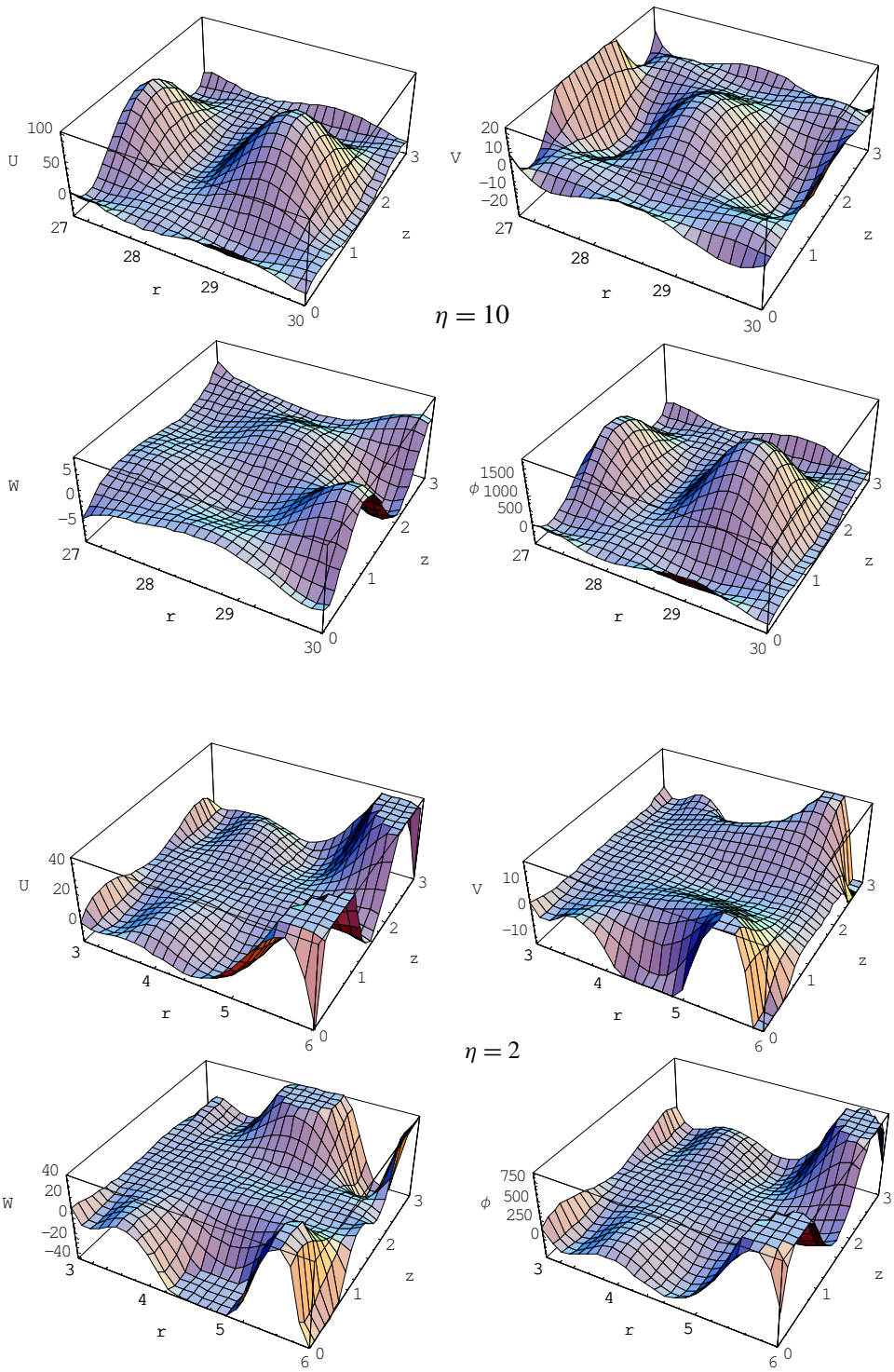

Figure 8. Displacement and electric potential profiles of the seventh mode for the Pr a-directional B/P/B-1/1/1 square ring at $kd = 30.3$. with $\eta = 10$ (top) and $\eta = 2$ (bottom).

to thickness ratio, the displacement and the electric potential of the Pr a-directional P/B/P-1/1/1 square ring with $\eta = 2$. The displacement and the electric potential are still mostly localized in the layers of PZT-4, but they become closer to the outer surface. In order to save space, above figures only show the displacement profile in the x direction. The displacement profiles in the other two directions show the same phenomena as the x direction displacement.

4. Conclusions

This paper proposed a double orthogonal polynomial series approach to solve wave propagation problems in 2-D multilayered piezoelectric rectangular rings. The dispersion curves, the displacement, and the electric potential shapes of various layered rectangular rings are obtained. According to the present numerical results, we can draw the following conclusions:

(a) Numerical comparison of the wave dispersion curves show that the double orthogonal polynomial method can accurately and efficiently solve the guided wave propagation problems in multilayered rectangular ring.

(b) The polarization direction and stacking sequence have weak influences on the dispersion curves, but radius to thickness ratio, volume fraction, and width to height ratio have significant influences on the dispersion curves. So, we can change the wave speed of the piezoelectric ring transducer through adjusting its thickness ratio, volume fraction and width to height ratio.

(b) The high frequency wave displacements and electric potential are mainly concentrated in the layer with a lower wave speed and they approach the outer surface of the ring with a little radius to thickness. Through changing the stacking sequence of the layered piezoelectric ring transducer, we can position the maximum displacement and electric potential where we want.

Acknowledgments

This work was supported by the National Natural Science Foundation of China (No. 11272115) and the Outstanding Youth Science Foundation of Henan Polytechnic University (No. J2013-08) and Science and Technology Agency of Henan Province (No. 144100510016), China.

References

[Adler 2000] E. L. Adler, "Bulk and surface acoustic waves in anisotropic solids", *Int. J. High Speed Electron. Syst.* **10**:03 (2000), 653–684.

[Ballandras et al. 2004] S. Ballandras, A. Reinhardt, V. Laude, A. Soufyane, S. Camou, W. Daniau, T. Pastureaud, W. Steichen, R. Lardat, M. Solal, and P. Ventura, "Simulations of surface acoustic wave devices built on stratified media using a mixed finite element/boundary integral formulation", *J. Appl. Phys.* **96**:12 (2004), 7731–7741.

[Cai et al. 2001] C. Cai, G. R. Liu, and K. Y. Lam, "A technique for modelling multiple piezoelectric layers", *Smart Mater. Struct.* **10**:4 (2001), 689–694.

[Chou et al. 1991] C. S. Chou, J. W. Yang, Y. C. Hwang, and H. J. Yang, "Analysis on vibrating piezoelectric beam gyroscope", *Int. J. Appl. Electrom. Mater.* **2**:3 (1991), 227–241.

[Collet 2004] B. Collet, "Recursive surface impedance matrix methods for ultrasonic wave propagation in piezoelectric multilayers", *Ultrasonics* **42**:1–9 (2004), 189–197.

[Datta and Hunsinger 1978] S. Datta and B. J. Hunsinger, "Analysis of surface waves using orthogonal functions", *J. Appl. Phys.* **49**:2 (1978), 475–479.

[Dökmeci 1974] M. C. Dökmeci, "A theory of high frequency vibrations of piezoelectric cyrstal bars", *Int. J. Solids Struct.* **10**:4 (1974), 401–409.

[Guo et al. 2009] Y. Q. Guo, W. Q. Chen, and Y. L. Zhang, "Guided wave propagation in multilayered piezoelectric structures", *Sci. China G Phys. Mech. Astronom.* **52**:7 (2009), 1094–1104.

[Kim and Hunt 1990] Y. Kim and W. D. Hunt, "Acoustic fields and velocities for surface-acoustic-wave propagation in multilayered structures: An extension of the Laguerre polynomial approach", *J. Appl. Phys.* **68**:10 (1990), 4993–4997.

[Lefebvre et al. 1999] J.-E. Lefebvre, V. Zhang, J. Gazalet, and T. Gryba, "Legendre polynomial approach for modeling free-ultrasonic waves in multilayered plates", *J. Appl. Phys.* **85**:7 (1999), 3419–3427.

[Ludwig and Lengeler 1964] W. Ludwig and B. Lengeler, "Surface waves and rotational invariance in lattice theory", *Solid State Comm.* **2**:3 (1964), 83–86.

[Maradudin et al. 1972] A. A. Maradudin, R. F. Wallis, D. L. Mills, and R. L. Ballard, "Vibrational edge modes in finite crystals", *Phys. Rev. B* **6**:4 (1972), 1106–1111.

[Mindlin and McNiven 1960] R. D. Mindlin and H. D. McNiven, "Axially symmetric waves in elastic rods", *J. Appl. Mech. (ASME)* **27**:1 (1960), 145–151.

[Nayfeh 1995] A. H. Nayfeh, *Wave propagation in layered anisotropic media: With applications to composites*, North-Holland Ser. Appl. Math. Mech. **39**, North-Holland, Amsterdam, 1995.

[Pastureaud et al. 2002] T. Pastureaud, V. Laude, and S. Ballandras, "Stable scattering-matrix method for surface acoustic waves in piezoelectric multilayers", *Appl. Phys. Lett.* **80**:14 (2002), 2544–2546.

[Taweel et al. 2000] H. Taweel, S. B. Dong, and M. Kazic, "Wave reflection from the free end of a cylinder with an arbitrary cross-section", *Int. J. Solids Struct.* **37**:12 (2000), 1701–1726.

[Wang and Rokhlin 2002] L. Wang and S. I. Rokhlin, "Recursive asymptotic stiffness matrix method for analysis of surface acoustic wave devices on layered piezoelectric media", *Appl. Phys. Lett.* **81**:21 (2002), 4049–4051.

[Wang and Rokhlin 2004] L. Wang and S. I. Rokhlin, "Modeling of wave propagation in layered piezoelectric media by a recursive asymptotic method", *IEEE Trans. Ultrason. Ferroelectr. Freq. Control* **51**:9 (2004), 1060–1071.

[Wu et al. 2014] B. Wu, W. Q. Chen, and J. Yang, "One-dimensional equations for coupled extensional, radial, and axial-shear motions of circular piezoelectric ceramic rods with axial poling", *Arch. Appl. Mech.* **84**:9-11 (2014), 1677–1689.

[Yu et al. 2012] J. G. Yu, J.-E. Lefebvre, Y. G. Guo, and L. Elmaimouni, "Wave propagation in the circumferential direction of general multilayered piezoelectric cylindrical plates", *IEEE Trans. Ultrason. Ferroelectr. Freq. Control* **59**:11 (2012), 2498–2508.

[Yu et al. 2013] J. G. Yu, J.-E. Lefebvre, and Y. Q. Guo, "Wave propagation in multilayered piezoelectric spherical plates", *Acta Mech.* **224**:7 (2013), 1335–1349.

[Zhang et al. 2001] V. Y. Zhang, J.-E. Lefebvre, C. Bruneel, and T. Gryba, "A unified formalism using effective surface permittivity to study acoustic waves in various anisotropic and piezoelectric multilayers", *IEEE Trans. Ultrason. Ferroelectr. Freq. Control* **48**:5 (2001), 1449–1461.

Received 11 Mar 2014. Revised 31 Jul 2015. Accepted 29 Nov 2015.

JIANGONG YU: yu@emails.bjut.edu.cn
School of Mechanical and Power Engineering, Henan Polytechnic University, Jaiozuo, 454003, China

XIAODONG YANG: 806607231@qq.com
School of Mechanical and Power Engineering, Henan Polytechnic University, Jiaozuo, 454003, China

JEAN-ETIENNE LEFEBVRE: jean-etienne.lefebvre@univ-valenciennes.fr
University of Lille Nord de France, F-59000 Lille, France, and, UVHC, IEMN-DOAE, F-59313 Valenciennes Cedex 9, France, and, CNRS, UMR 8520, F-59650 Villeneuve d'Ascq, France

JOURNAL OF MECHANICS OF MATERIALS AND STRUCTURES

msp.org/jomms

Founded by Charles R. Steele and Marie-Louise Steele

See msp.org/jomms for submission guidelines.

JoMMS (ISSN 1559-3959) at Mathematical Sciences Publishers, 798 Evans Hall #6840, c/o University of California, Berkeley, CA 94720-3840, is published in 10 issues a year. The subscription price for 2016 is US $575/year for the electronic version, and $735/year (+$60, if shipping outside the US) for print and electronic. Subscriptions, requests for back issues, and changes of address should be sent to MSP.

JoMMS peer-review and production is managed by EditFLOW® from Mathematical Sciences Publishers.

PUBLISHED BY

mathematical sciences publishers

nonprofit scientific publishing

http://msp.org/

Journal of Mechanics of Materials and Structures

Volume 11, No. 3 May 2016